Cloud removal of Gaofen-5 VNIR hyperspectral data using auxiliary multispectral data via residual neural networks

Mingyuan Peng (1)(2), Lifu Zhang (1), Xuejian Sun (1), Yi Cen (1)

[1] Institute of Remote Sensing and Digital Earth, Chinese Academy of Sciences, 20 Datun road, Chaoyang District, Beijing, 100101, China
[2] University of Chinese Academy of Sciences, 19 Yuquan Road, Shijingshan District, Beijing, 100049, China

Email: pengmy@radi.ac.cn; zhanglf@radi.ac.cn; sunxj@radi.ac.cn

KEY WORDS: Cloud removal; Residual Neural Networks; GF-5; Hyperspectral Data

ABSTRACT: Gaofen-5 (GF-5) is a newly launched satellite with 6 types of payloads, one of which is the Advanced Hyperspectral Imager (AHSI), a hyperspectral VNIR sensor with spectral range from 0.4μm-2.5μm and its spectral resolution is 5nm. As most sensors, its data suffers from the contamination of clouds. In thick cloud regions on particular days, the data are not accessible in particular thick cloud regions, which hinders its wider applications. Here we propose a thick cloud removal method of GF-5 hyperspectral VNIR data with the aid of corresponding cloud-free multispectral data via residual neural networks (ResNet). The basic idea is to build nonlinear mapping between hyperspectral data and multispectral data via residual neural networks and use the mapping to restore the cloud-contaminated data. First the clouds in the scene are detected and set as cloud regions, and then the residual neural networks are trained with cloud-free regions of hyperspectral data and multispectral data. Finally, the cloud regions are calculated using corresponding cloud-free multispectral data to derive the cloud removed hyperspectral data. The method is tested with simulated data derived from GF-5 and yields accurate results.

1. INTRODUCTION

Remote sensing are, nowadays, used widely in different applications such as forestry, agriculture, geology and etc. Prior to all these applications, the first step of all these applications is to obtain remote sensing data. However, due to bad weather conditions, the remote sensing data usually suffers from cloud contamination. This greatly hinders the remote sensing applications, especially when the scene is contaminated by thick clouds in the visual and near-infrared range(Lin, et al., 2013), which means the clouded area has no information contained. Although the smaller revisiting time makes it possible to obtain many data in one certain region, there are still gaps between available data, bringing difficulties to applications such as long-term monitoring.

Gaofen-5 (GF-5) satellite is the only terrestrial environment hyperspectral observation satellite in China's high-resolution geospatial major science and technology special plan, and the world's first atmospheric and terrestrial integrated hyperspectral observation satellite. It is a newly launched in 2018 and is equipped with 6 payloads covering ultraviolet to long-wave infrared, including the Advanced Hyperspectral Imager (AHSI), Visual and Infrared Multispectral Sensor (VIMS), Greenhouse-gases Monitoring Instrument (GMI), Atmospheric Infrared Ultraspectral (AIUS), Environment Monitoring Instrument (EMI), Directional Polarization Camera (DPC). Among these equipment, AHSI is the first hyperspectral data with both wide swath and wide spectral range of 0.4μm-2.5μm and

its spectral resolution is 5nm. As GF-5 fight height is 705 km, it also suffers from the contamination of clouds, which brings obstacles to its wide applications.

One solution to this problem is cloud removal of the remote sensing data. To date, there are many researches on cloud removal of remote sensing images, and they can be divided into three categories(Cheng, et al., 2014). One is the non-complementation approaches, which is to reconstruct the cloud-contaminated area using the remaining parts of the images without the aid of other scenes(Chen, et al., 2005, Lorenzi, et al., 2011, Maalouf, et al., 2009). The missing data are synthesized by propagating the geological structure in the region. Although this method can obtain a relatively good visual result, the accuracy of this method is questionable and hinders its quantitative applications especially when it comes to hyperspectral data. Other category is the complementation approaches, which is to utilize the clean and complete auxiliary band of data to restore the cloud contaminated data (Li, et al., 2012, Rakwatin, et al., 2009, Travis, 2009). This is usually done by modelling the relationship between the cloud contaminated data and the auxiliary band of data. This method can obtain a relatively better result than the first method, yet it highly depends on the spectral compatibility(Lin, et al., 2013), and more applicable to remove haze or thin clouds. Another category is the multi-temporal approaches, which is to use the overlapped data from other time to restore the missing data (Gabarda and Cristóbal, 2007, Jiao, et al., 2007, Melgani, 2006, Zeng, et al., 2013). The third approach tends to yield most accurate results, but when the temporal gap is too large or the atmospheric conditions are quite different, the results may suffer from spectral differences. Also, there are few researches on cloud removal of hyperspectral data, most of which focus mainly on preserving the spectral information, ignoring maintaining the spatial information.

To overcome the problems mentioned above, here we propose the method of cloud removal of GF-5 hyperspectral data using the residual neural networks. First, the cloud area of GF-5 hyperspectral data are detected and a cloud mask result is yielded. Then, the cloud mask is applied on the hyperspectral data and multispectral data to obtain data of the overlapped cloud-free area, and nonlinear mapping is modeled and trained via residual neural networks. And last, the clouded area of hyperspectral data are predicted based on the relationship and auxiliary multispectral data. The method is able to remove thick clouds in a relatively large area and yields excellent results in both preserving spectral and spatial results.

2. PROPOSED METHOD

2.1 Basic Hypothesis of the Proposed Method

The basic hypothesis of the proposed method is that the mappings between hyperspectral data and multispectral data of the same scene is nonlinear and transferable to cloud-contaminated area when land covers would not change during a short period of time. On top of that, we can model the relationship between the cloud-free areas of GF-5 hyperspectral data and the auxiliary clean multispectral data on nearby date, and utilize the relationship to predict the cloud-contaminated area. Here we represent the Gf-5 hyperspectral data as H, the cloud-contaminated and cloud-free area of which is H_c and H_f. We also note the auxiliary multispectral data as M, the overlapped area with H as M_o. Modelling the relationship between them can be represented as

$$\mathrm{H}_f = \mathrm{F}(\mathrm{M}_o)$$

And according to the hypothesis that land cover types is invariable, we can get

$$\mathrm{H} = \mathrm{F}(\mathrm{M})$$

They share the same relationship $\mathrm{F}(\cdot)$.As hyperspectral data is huge in volume and tends to have redundancy between bands, here we perform principle components to reduce the dimension. Thus, modelling the relationship between

dimensionally reduced hyperspectral data H' and the auxiliary multispectral data M becomes getting function G by solving

$$H_f{}' = G(M_o) \rightarrow H' = G(M)$$

where $H_f{}'$ represents the principal components of the cloud-free area of the hyperspectral data.

2.2 The Structure of Cloud Removal Model

For learning the relationship F, here we use the technique of residual neural network. Research shows that the residual learning is easier to optimize compared to plain CNN networks. Rather than learning the nonlinear mapping of H(x), which can be represented in a form of F(x)+x, residual learning learns its residual F(x). The mapping can be represented as

$$y = \mathcal{F}(x, \{W_i\}) + W_s x$$

in which x represents the input of a certain layer, y represents the output of this layer. The residual learning can be realized by the structure of "short connections", which are those skipping some layers (Bishop, 1995, He, et al., 2016). Short connections are the outputs of identity mapping added to outputs of the stacked layers as shown in the Figure 1. The residual learning is a useful preconditioning to identity mapping. If the optimal function is close to an identity mapping, it should be easier to learn the perturbations from identity mapping than to learn the optimal function in a new one(He, et al., 2016), thus it's easier to optimize than plain networks. In our case, the residual block is piled with convolutional layers, batch normalization layers and leaky ReLU layers.

The following figure shows the structure of the model which is piled with loads of residual blocks. The input data is the multispectral data and the output data is the principle components of the GF-5 hyperspectral data. For the inputs and outputs of the model, we divide the data into small patches, each patches overlap by half to diminish the distortion on the edge of each patches during restoration.

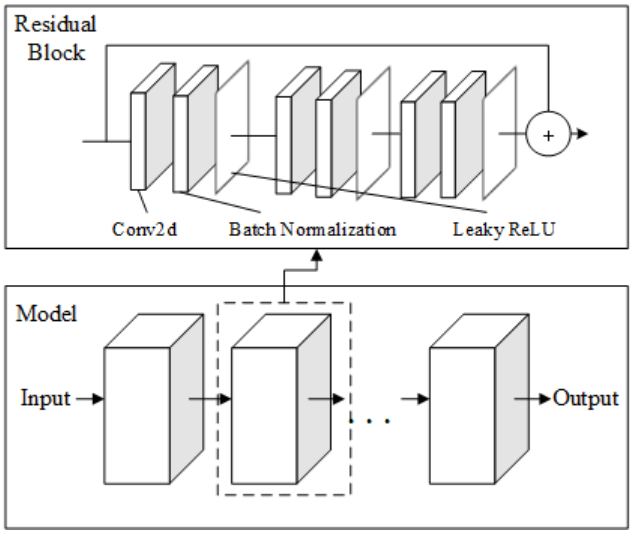

Figure 1. The structure of residual block and the model

2.3 Main Process of Cloud Removal of GF-5 VNIR Hyperspectral Data

The main process of the cloud removal of GF-5 hyperspectral data is shown in the figure below. First the clouded hyperspectral data is transformed using principal component analysis, and is used to generate cloud mask. Here we use the K-Means method to generate approximate estimation of the cloud mask. Then the cloud mask, PCA transformed hyperspectral data and multispectral data are used to generate the training patch pairs. Here the

hyperspectral data and auxiliary multispectral data are divided into small patches as training patches. The patch is discarded if there exist any cloud in the patch. After obtaining training patches, the ResNet model is trained to get the nonlinear mapping F(·) between GF-5 hyperspectral data and the auxiliary multispectral data. Finally the cloud area was predicted and restored using the trained models.

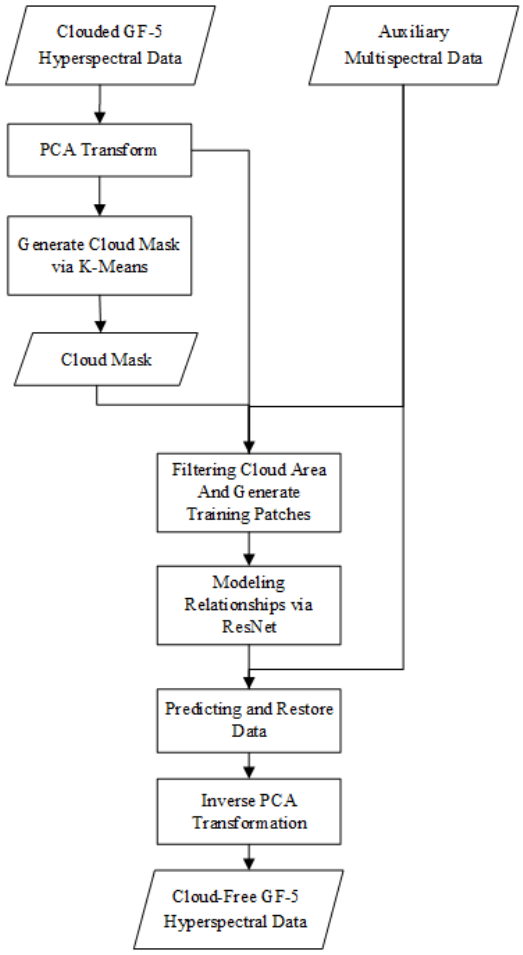

Figure 2. Flowchart of the method

3 EXPERIMENTS AND RESULTS

3.3 Test Dataset

The test scene of GF-5 hyperspectral data was obtained in Germany, on May 29th, 2018. It possesses 1024 pixels in lines and 768 pixels in columns with 180 bands ranging from 390.12 nm to 1028.98 nm. The test scene is mainly covered by crop fields. The data was processed with QUick atmospheric correction and noise reduction using principal component analysis by ENVI 5.2. Then the test data was added clouds which was derived from other scenes of GF-5 hyperspectral data and cloud cover is approximately 0.249. Figure 3 and Figure 4 show the RGB composites of the original and synthetic hyperspectral data and Figure 5 shows several spectra of the added cloud.

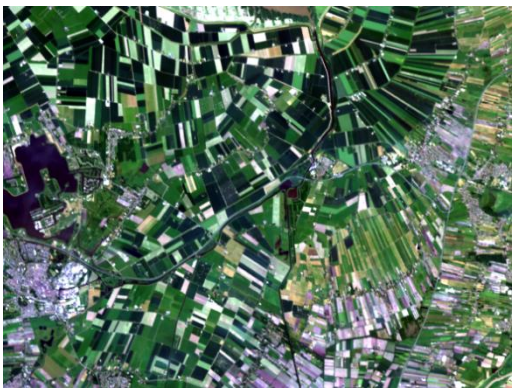

Figure 3. Original GF-5 hyperspectral data

Figure 4.Sythesized GF-5 data with cloud

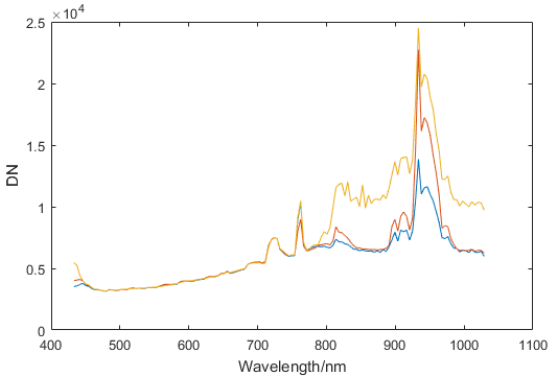

Figure 5. Cloud spectra of the test data

The auxiliary multispectral data is the Sentinel-2a multispectral data obtained on May 28th, 2018. We chose the 7 bands of the data with spatial resolution of 20m ranging from 492.1nm to 864.0nm. Also, the auxiliary data was possessed with QUick atmospheric correction by ENVI 5.2.

3.4 Experimental Settings

The whole process was processed by Keras 2.0 in python. The number of residual blocks of the ResNet structure was set as 10. The patch size was set to be 8×8 pixels per patch. The training epoch was set to be 1000. The optimizer was set to be the Adam and the learning rate was set to be 0.001. We also used the strategy of early stopping to end the training process when training loss does not further reduce. This can avoid the overfitting of the ResNet model.

3.5 Results

To evaluate the effectiveness of this method, the result was assessed by visual interpretation and quantitative assessments. The figure below shows the overall and detail scene of RGB composites of the cloud removal result in the cloud-blocked scenes. We can see from the result that the clouds have been completely removed, and the spatial details of the data is well preserved. Also, we collected spectra of the cloud blocked area from original scene and the restored scene and they are shown in the figure below. The similarity of the corresponding spectra shows the ability of this method to restore the spectral information of the blocked area.

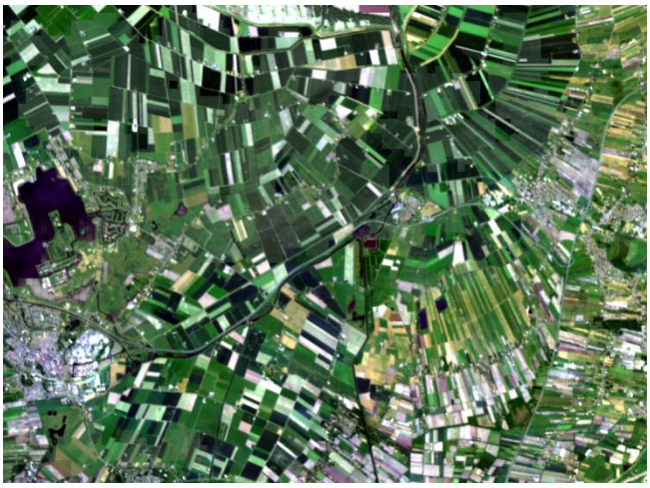

(a)

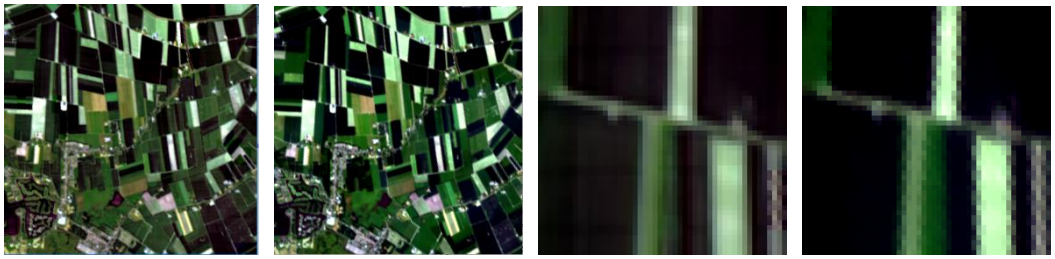

(b) (c) (d) (e)

Figure 6. Cloud removed results in spatial domain (RGB composites)

(a. Whole scene of the restored area b. original data c. restored data d. original data e. restored data)

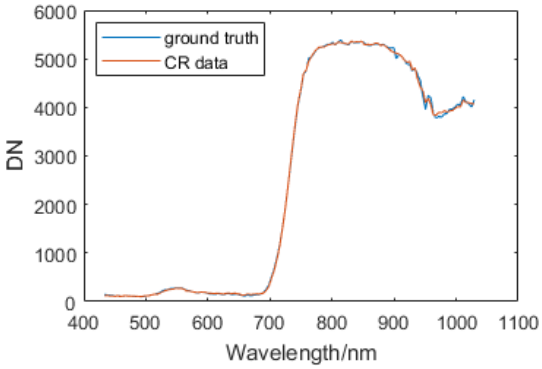

(a)

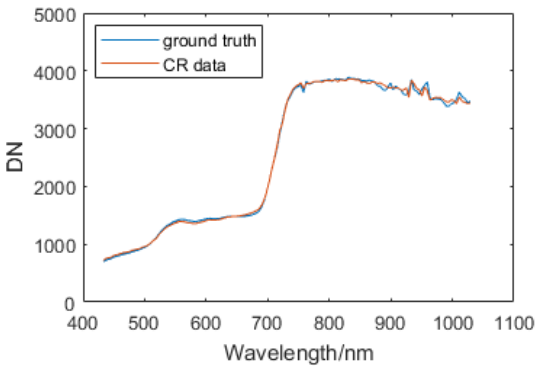

(b)

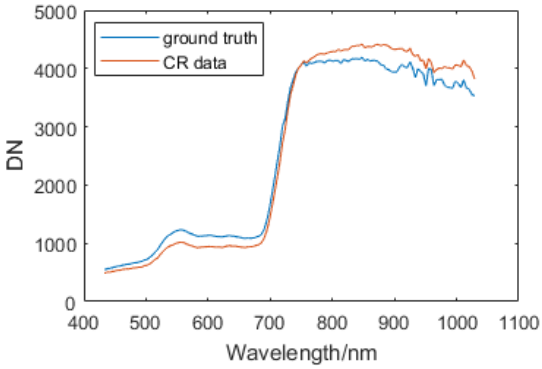

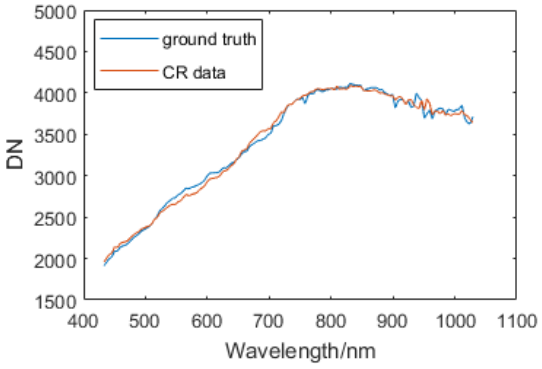

(c) (d)

Figure 7. Spectra of typical land covers of original and cloud-removed data

For the quantitative assessment we used the quality indices of PSNR, CC, RMSE and SAM to evaluate the results with the original GF-5 hyperspectral data. The restored data was calculated with the original data in the whole scene. The following figure shows the indices before and after the cloud removal procedures. As we can see in the figure, SAM decreases from 7.09 to 1.93, which shows the spectral feature was restored and close to the original hyperspectral data. PSNR increases from 19.39 to 37.11, RMSE decreases from 1595.1 to 267.62, CC increases from 0.356 to 0.965 which shows the restoration accuracy has been increased.

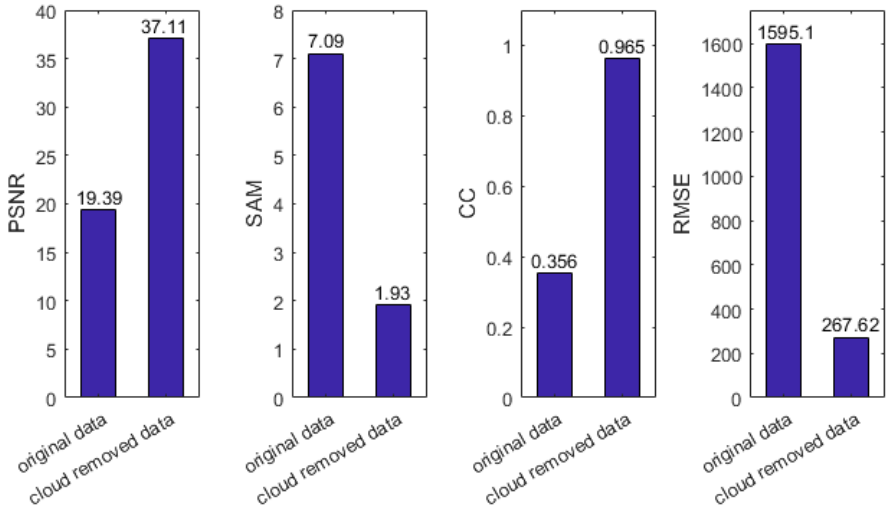

Figure 8. Quantitative assessment of clouded and cloud-removed data

4 CONCLUSIONS

Here a method for cloud removal of GF-5 hyperspectral data using residual neural networks with aid of the auxiliary multispectral data is proposed. The method is to build the nonlinear mapping using ResNet between the principle components of GF-5 hyperspectral data and the auxiliary multispectral data, and use the mapping to predict the data from cloud-contaminated area. The method is tested through synthetic clouded GF-5 hyperspectral data and Sentinel-2 multispectral data. Results show that this method can accurately restore the hyperspectral data of the cloud-contaminated area even when the data is blocked by thick clouds, and the method can also improve the quality of the cloud-contaminated data in both spectral and spatial information.

REFERENCE

Bishop C. M., 1995. Neural Networks for Pattern Recognition. Agricultural Engineering International the Cigr Journal of Scientific Research & Development Manuscript Pm, 12, pp. 1235 - 1242

Chen F., Zhao Z., Ling P. and Yan D., 2005. Clouds and cloud shadows removal from high-resolution remote sensing images. IEEE International Geoscience & Remote Sensing Symposium, pp.

Cheng Q., Shen H., Zhang L., Yuan Q. and Chao Z., 2014. Cloud removal for remotely sensed images by similar pixel replacement guided with a spatio-temporal MRF model. Isprs Journal of Photogrammetry & Remote Sensing, 92, pp. 54-68

Gabarda S. and Cristóbal G., 2007. Cloud covering denoising through image fusion ☆. Image & Vision Computing, 25, pp. 523-530

He K., Zhang X., Ren S. and Sun J., 2016. Deep Residual Learning for Image Recognition. 2016 IEEE Conference on Computer Vision and Pattern Recognition (CVPR), pp. 770-778

Jiao Q., Luo W., Liu X. and Zhang B., 2007. Information reconstruction in the cloud removing area based on multi-temporal CHRIS images. pp.

Li H., Zhang L., Shen H. and Li P., 2012. A Variational Gradient-based Fusion Method for Visible and SWIR Imagery. Photogrammetric Engineering & Remote Sensing, 78, pp. 947-958

Lin C. H., Tsai P. H., Lai K. H. and Chen J. Y., 2013. Cloud Removal From Multitemporal Satellite Images Using Information Cloning. IEEE Transactions on Geoscience & Remote Sensing, 51, pp. 232-241

Lorenzi L., Melgani F. and Mercier G., 2011. Inpainting Strategies for Reconstruction of Missing Data in VHR Images. IEEE Geoscience & Remote Sensing Letters, 8, pp. 914-918

Maalouf A., Carre P., Augereau B. and Fernandez-Maloigne C., 2009. A Bandelet-Based Inpainting Technique for Clouds Removal From Remotely Sensed Images. IEEE Transactions on Geoscience & Remote Sensing, 47, pp. 2363-2371

Melgani F., 2006. Contextual reconstruction of cloud-contaminated multitemporal multispectral images. IEEE Transactions on Geoscience & Remote Sensing, 44, pp. 442-455

Rakwatin P., Takeuchi W. and Yasuoka Y., 2009. Restoration of Aqua MODIS Band 6 Using Histogram Matching and Local Least Squares Fitting. IEEE Transactions on Geoscience & Remote Sensing, 47, pp. 613-627

Travis D. J., 2009. Restoration of clouded pixels in multispectral remotely sensed imagery with cokriging. International Journal of Remote Sensing, 30, pp. 2173-2195

Zeng C., Shen H. and Zhang L., 2013. Recovering missing pixels for Landsat ETM+ SLC-off imagery using multi-temporal regression analysis and a regularization method. Remote Sensing of Environment, 131, pp. 182-194